XIV National School on Superconductivity, Ostrów Wielkopolski, October 13–17, 2009

Magnetic Nature of a Ni Dopant in $La_{1.85}Sr_{0.15}CuO_4$: Spin-Glass Behavior

A. Malinowski*, V.L. Bezusyy, R. Minikayev, W. Paszkowicz, P. Dziawa, Y. Syryanyy and M. Sawicki

Institute of Physics, Polish Academy of Sciences, al. Lotników 32/46, 02-668 Warsaw, Poland

The magnetic properties of $La_{1.85}Sr_{0.15}CuO_4$ doped with Ni was investigated in the field up to 5 T and in the temperature range from 2 K to 400 K using both dc and ac techniques. For Ni content larger than 0.05 the system exhibits irreversibility of low-field susceptibility $\chi(T)$ below a certain temperature depending on y and a cusp at T_g in $\chi(T)$ measured after zero-field cooling. The decay of remnant magnetization below T_g with time is described by a stretched-exponential function. In accordance with scaling theory, all the $\chi(T)$ data for $y = 0.50$ sample taken in the vicinity of T_g at different fields collapse onto two separate curves when plotted as $q|t|^{-\beta}$ vs. $B^2|t|^{-\beta-\gamma}$, where q is the spin-glass order parameter, $t = (T - T_g)/T_g$, and β and γ are the critical exponents. All these features taken together reveal existence of spin-glass phase below T_g. Variation of T_g with y is linear below $y = 0.25$ and T_g extrapolates to 0 K for $y \to 0$ what strongly suggests that spin-glass phase extends into superconducting region of the phase diagram.

PACS numbers: 74.62.Dh, 75.40.Cx, 75.40.Gb, 75.50.Lk

1. Introduction

The nature of the state out of which the superconductivity arises is still one of the unresolved issues in the physics of cuprates. Different impurities, magnetic and non-magnetic ones, introduced into Cu–O planes are used to suppress the superconductivity in these systems with the hope to reveal the features of the normal state. The intriguing Ni dopant have attracted the attention from the beginning of high-T_C superconductivity. Nominally magnetic Ni^{2+} ion ($3d^8$, $S = 1$) is known to have a weaker effect on superconductivity than nominally non-magnetic Zn^{2+} ($3d^{10}$, $S = 0$) ion. As regard to electrical transport in the normal state, quasiparticle scattering at Ni was found to be predominantly non-magnetic [1]. Based on c-axis optical conductivity measurements in underdoped $NdBa_2Cu_3O_{6.8}$ it was claimed that Ni strongly enhances the pseudogap energy [2]. On the other hand, it was suggested that for small concentrations Ni is substituted as Ni^{3+} ion [3]. If so, this may mean that Ni just shifts the system towards the smaller hole concentration in the cuprate phase diagram (where the temperature of the opening of pseudogap is larger) what is effectively observed as enhancement of the pseudogap. Just recently, Ni was claimed to not disturb the antiferromagnetic (AF) spin-1/2 network in Cu–O planes for concentrations smaller than the hole concentration in the system [4]. The measurements of local distortions around Ni ions replacing Cu ions in $La_{2-x}Sr_xCuO_4$ (LSCO) suggest that for these small concentrations Ni serves only as a hole-absorber and creates a strongly hole-bond state with the effective moment $S = 1/2$ that couples antiferromagnetically with $S = 1/2$ moments of the surrounding Cu ions. Based on this, a magnetic-impurity picture for Ni dopant in superconducting cuprates was completely disqualified [4]. Our study shows that so definitive statement is not correct. Ni behaves as magnetic impurity in LSCO system and frustrates the AF order in the Cu–O planes even for the smallest concentration.

2. Experiment details

The polycrystalline samples of $La_{1.85}Sr_{0.15}Cu_{1-y}Ni_yO_4$ (LSCNO) were synthesized by means of a conventional solid-state reaction method. The stoichiometric amounts of pure La_2O_3, $SrCo_3$, CuO and NiO powders were carefully mixed and pressed into pellets. The pellets were sintered in a pure oxygen gas flow at 1320 K for 48 h and then cooled down to room temperature with the rate 2 K/min. Next, the samples were grinded, pressed back into pellets and sintered in the identical way again. In total, the whole procedure was repeated three times. The DC and AC magnetic measurements in the field up to 5 T and in the temperature range from 2 K up to 400 K were carried out with the use of the commercial SQUID magnetometer (MPMS, Quantum Design).

3. Results and discussion

The dc magnetic susceptibility, χ, vs. T curves measured at low, 10 Oe, field exhibit branching below a characteristic temperature T_{irr}. Magnetization depends on the thermal-magnetic history of the sample and difference between zero-field cooling (ZFC) and field cooling

* corresponding author; e-mail: artur.malinowski@ifpan.edu.pl

(FC) mode is clearly seen in the system — see Fig. 1. Such a behavior is commonly taken as a fingerprint for the spin-glass systems. However, the difference between ZFC and FC mode occurs not only in "canonical" spin glasses (SG) but in superparamagnetic and cluster-spin systems as well (and even in conventional ferromagnets with broad distribution of potential barriers). In the case of superparamagnets, below the blocking temperature T_b of *independent* superparamagnetic entitles (either single ions or clusters) the FC magnetization continues to increase with decreasing temperature, while for LSCNO we observe relatively flat magnetization below the bifurcation temperature of $\chi(T)$ curve. However, when the interaction between single entities occurs in the superparamagnetic system, it can be difficult to distinguish between such an *interacting* superparamagnet and a real spin glass exhibiting a thermodynamic phase transition [5]. Let us note that the temperature of maximum in the ZFC $\chi(T)$ curve, T_g, is slightly below T_{irr} (in Fig. 1 marked for $y = 0.25$ sample) while in the canonical SG usually $T_{irr} \lesssim T_g$ [6]. The difference between T_g and T_{irr} increases with Ni content and is especially clearly seen in the samples with Ni content larger than for these depicted in Fig. 1. For "pure" nicklate, i.e. for $y = 1$, $T_g = 23.5$ K while the bifurcation point in $\chi(T)$ curve is located at 80 K (not shown here). This can be a manifestation of spin clusters presence in the system [7]. The temperature T_g increases linearly with Ni content, at least up to $y = 0.25\%$, and extrapolates to zero for $y = 0$ (see inset to Fig. 1). For small Ni content, T_g is outside our measurement window and/or is masked by the onset of superconductivity. However, the result of this linear extrapolation strongly suggests that Ni frustrates AF order in the Cu–O planes of LSCNO starting from its smallest concentration.

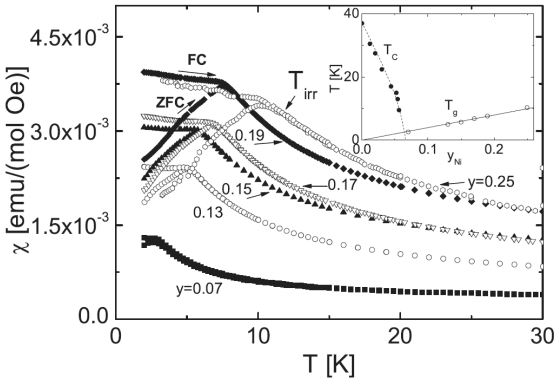

Fig. 1. Susceptibility of selected LSCNO samples measured at 10 Oe, both in ZFC and FC mode. Inset: the temperatures of transition to superconducting phase, T_C, and to spin-glass phase, T_g, as a function of Ni content. The solid line is the best fit to T_g vs. T data for $y \leq 0.25$. The dashed line is a guide to the eye.

To obtain a more detailed insight into dynamics of the phase below T_g we measured the frequency dependence of ac susceptibility. In Fig. 2 we depicted the real part of ac susceptibility, χ', for $y = 0.25$ sample, normalized to the value at 1 Hz. At 25 K, i.e. at the temperature well above T_g, in the paramagnetic state, variation of f over three decades does not influence on χ' in a noticeable way. Below T_g, the χ' exhibits a logarithmic frequency dependence. Such a frequency dependence was observed for many SG systems [8]. However, it is not unique for SG but rather exists in any disordered system with a broad distribution of the activation barrier heights [9].

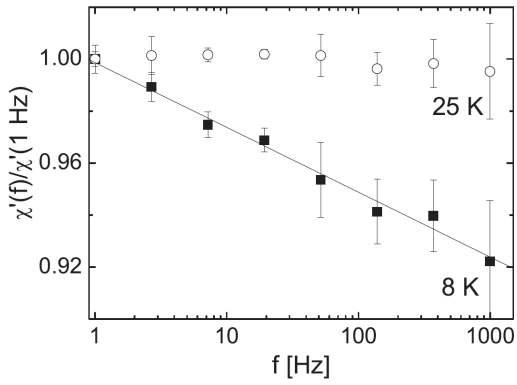

Fig. 2. The real part of the ac susceptibility of $y = 0.25$ sample at 8 K and 25 K. The amplitude of ac field was 1 Oe and the measurements were carried out in 10 Oe dc field. The solid line is the best fit to logarithmic frequency dependence of χ'.

In the temperature dependence of χ' there is a sharp cusp observed near T_g. The imaginary part of ac susceptibility, the absorption χ'', appears only below T_g. The position of the cusp in $\chi'(T)$, T_f, corresponds to the maximum slope in $\chi''(T)$ and shifts to higher temperature with increasing frequency, while the magnitude of $\chi'(T_f)$ decreases for higher frequency. This is a behavior expected for a spin-glass system. A measure of this frequency dependence is the parameter $\delta = \Delta T_f/(T_f \Delta \ln \omega)$ [10]. For $y = 0.25$ ($y = 0.50$) sample we obtained $\delta = 0.012$ ($\delta = 0.011$). These values are intermediate between those for superparamagnetic systems with noninteracting particles ($\delta \approx 0.1$) and those measured in the canonical spin systems (e.g. in CuMn $\delta \approx 0.002$), where interaction between spins weakens sensitivity to frequency [11, 12]. The values of $\delta \approx 0.01$ are typical for cluster glasses, i.e. systems with randomly distributed interacting magnetic clusters [13].

On the other hand, in the case of ferromagnetic or canted AF clusters in the system, a hysteresis is expected with large initial susceptibility because clusters at first saturate along their local easy axis and only after that became aligned with the applied field [7]. In LSCNO we observe a different behavior. The isothermal $M(H)$ curves which we measured below T_g after ZFC procedure have an "S" shape, i.e. the initial dM/dH is smaller than the slope at inflection point at a certain finite field. An example of such a curve is depicted in Fig. 3. Such a

behavior is typical for SG in the frozen state [10]. No trace of saturation is visible even at 5 T and 2 K and the measured magnetic moment calculated per Ni ion is very small. The virgin curve lies outside the hysteresis loop which suggests the presence of metastable states in the system. This "S"-shaped $M(H)$ curve smoothly evolves to linear dependence above $T_{\rm g}$.

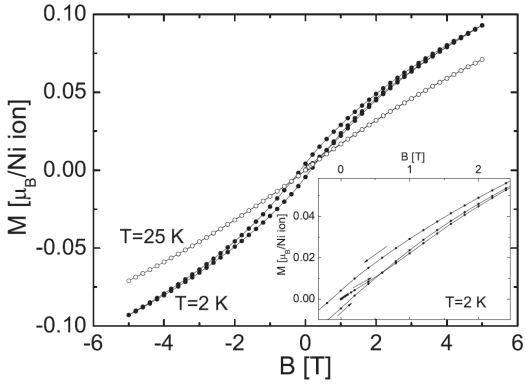

Fig. 3. The hysteresis loops for $y = 0.25$ sample measured at 2 K and 25 K. Inset shows the details of 2 K curve at small fields.

The presence of metastable states below $T_{\rm g}$ is clearly confirmed by the decay of remnant magnetization. We applied a magnetic field of 1000 Oe at 200 K, cooled the samples down to 2 K ($\approx$ 80 min), kept the temperature constant for 10 min and switched off the field. Next the thermoremanent magnetization, $M_{\rm TRM}$, was measured vs. time at $T = 2$ K and the results for $y = 0.25$ sample are presented in Fig. 4. $M_{\rm TRM}(t)$ appears to be well described by a stretched exponential formula, $M_{\rm TRM}(t) = M_0 \exp(-(t/\tau)^{1-n})$. This form is commonly used to describe different relaxation phenomena in different complex random systems with a distribution of relaxation times and, among others, was theoretically predicted for spin-glass systems as well [14]. The best fit was obtained for $1 - n = 0.32 \pm 0.01$, in perfect agreement with the numerical simulations on a 3-dimensional Ising SG [15]. The same value was found for non-doped LSCO system but the experiment time was not sufficient to exclude different types of $M_{\rm TRM}(t)$ dependences [16], while in pure nicklate, $La_{2-x}Sr_xNiO_4$, the time dependence of TRM was found to be inconsistent with a stretched exponential formula.

The last feature we use to identify the SG phase in LSCNO system is the scaling behavior. The analysis was carried out for $y = 0.50$ sample. For this sample, as for all others with Ni content larger than 0.07 (except pure nicklate, $y = 1$) the temperature-dependent part of χ above $T_{\rm g}$, $\chi - \chi_0$, is well described by the Curie–Weiss (CW) formula with negative θ ($\theta = -(5.0 \pm 0.2)$ K for $y = 0.50$). In the standard manner we define an SG order parameter, q, being a measure of data deviation from this CW dependence at lower temperature and higher field,

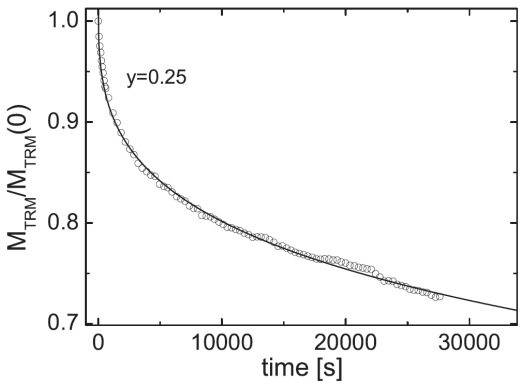

Fig. 4. The remnant magnetization of $y = 0.25$ sample measured at 2 K as a function of time after the field is switched off. The solid line is the best fit to a stretched exponential formula (see text).

$$\chi - \chi_0 = \frac{C}{T - \theta}(1 - q)\,. \tag{1}$$

The way in which q goes to zero when temperature approaches the SG transition temperature, $T_{\rm g}$, is described by the critical exponent β,

$$q \propto \mid t \mid^{\beta}, \tag{2}$$

where t is the reduced temperature $(T - T_{\rm g})/T_{\rm g}$. Fitting this formula to the FC data yields parameters ($\beta = 1.08 \pm 0.01$, $T_{\rm g} = 13.4 \pm 0.1$) different from these obtained for the ZFC data ($\beta = 0.63 \pm 0.03$, $T_{\rm g} = 12.7 \pm 0.1$) (see Fig. 5). Since the state of the system below $T_{\rm g}$ both after ZFC and FC procedure *is not* a state of thermodynamic equilibrium (and this explains the differences between the fit parameters) it is reasonable to take the averages as the experimentally measured values [16]. Let us note that the critical exponent $\beta = 0.9 \pm 0.2$ found in this way is close to the value $\beta = 1$ predicted by the mean field model and does not differ much from the values measured in the canonical SG (for instance in very dilute Ag:Mn exactly the same $\beta = 0.9 \pm 0.2$ was found [17]). The theory of critical phenomena predicts that right at the transition temperature $T_{\rm g}$ the order parameter q at large fields depends on the square of a uniform applied field as [18]

$$q \propto (B^2)^{1/\delta}. \tag{3}$$

We made a crossing of $q(T)$ curves taken at various constant fields in the FC mode (presented in Fig. 5) at the temperatures in the vicinity of the obtained $T_{\rm g} = 13.1 \pm 0.4$. Equation (3) was found to describe the data well and the best linear fit at $T_{\rm g}$ and higher fields on $\log q$ vs. $\log B$ scale yields the critical exponent $\delta = 6.0 \pm 0.1$. The divergence of the susceptibility at $T_{\rm g}$ is described by another critical exponent, γ, as $\chi \propto \mid T - T_{\rm g} \mid^{-\gamma}$ and the value of γ can be obtained via the scaling relationship [18]

$$\gamma = \beta(\delta - 1)\,. \tag{4}$$

Using the obtained β and δ we found $\gamma = 4.4 \pm 1.1$. In the canonical SG usually smaller values of $\gamma \approx 3$ were reported (see Table 8.2 in Ref. [18]) but in the SG phase of

LSCO without any impurities in the Cu–O planes similar $\gamma = 4.4 \pm 1.1$ was measured [16].

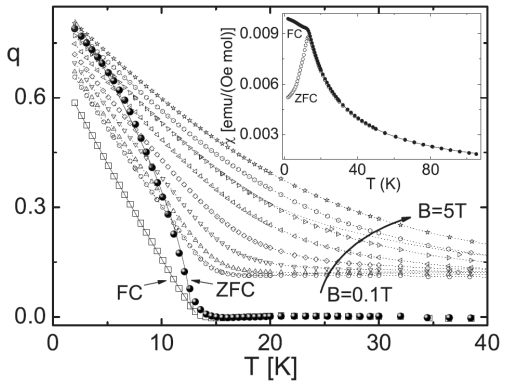

Fig. 5. The SG order parameter for $y = 0.50$ sample as a function of temperature at different fields B. The large symbols denote FC (open squares) and ZFC (solid spheres) data measured at $B = 10$ Gs while the small symbols represent the FC data collected at 0.1, 0.2, 0.5, 1, 2, 3, 4 and 5 T (from bottom to top) in the FC mode. The solid lines are the best fits to $q \propto t^{\beta}$ dependence (see text) and the dotted lines are the guides for eye only. In the inset the susceptibility of this sample measured in FC and ZFC mode is shown. The solid line is the best fit of the FC data above 15 K to the Curie–Weiss formula.

The scaling relation for the order parameter reads

$$q = \mid t \mid^{\beta} f_{\mp}\left(\frac{B^2}{\mid t \mid^{\beta+\gamma}}\right), \tag{5}$$

where f_- (f_+) is the scaling function for reduced temperature $t < 0$ ($t > 0$) [19–21]. Thus it is convenient to present the data at different fields in the vicinity of T_g as $q/\mid t \mid^{\beta}$ vs. $B^2/\mid t \mid^{\beta+\gamma}$. All the data collapse onto two separate curves, one for $t < 0$ (i.e. for temperatures below T_g) and second for $t > 0$, as it can be clearly seen in Fig. 6. At small B and T the q vs. T dependence becomes this described by the relationship given by Eq. (2) which in Fig. 5 is visible as the flattening of the upper curve (i.e. for $t < 0$). When temperature approaches T_g, regardless of from what side it takes place, both curves on the log–log scale asymptotically approach the straight line given by Eq. (3).

The scaling illustrated in Fig. 6 is sometimes used as a proof of a true three-dimensional (3D) SG transition [16]. However, similar scaling plots (resembling the curve for $T > T_g$ in Fig. 6) with *finite* critical temperature T_c was obtained in Monte Carlo simulations for two-dimensional (2D) Edwards–Anderson Ising SG with a nearest-neighbor Gaussian exchange distribution, for which no finite-temperature transition exists [18, 22]. To be more precise: although $T_c = 0$ was shown to be the correct choice, the numerical data appeared to be consistent with 3D scaling expressions (distinguished from 2D case by *finite* $T_c > 0$) equally well [22]. Measurements carried out on the experimental realization of the

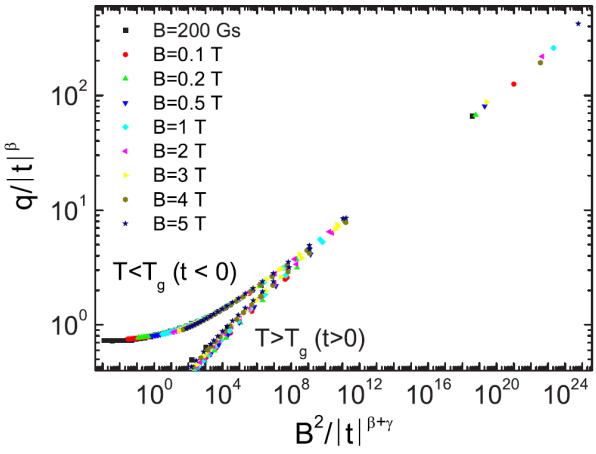

Fig. 6. The scaling plot of the susceptibility of LSCNO sample with $y = 0.5$ Ni content depicted with the help of the order parameter q at different fields and temperatures below ($t < 0$) and above ($t > 0$) $T_g = 13.1$.

model described in Ref. [22], namely $Rb_2Cu_{1-x}Co_xFe_4$, gave $\beta = 0.0 \pm 0.1$ in accordance with the theory and the obtained data exhibit $T_c = 0$ scaling. However, the data could be also scaled to a 3D expression (although there is a small trend towards the better fits with lower T_c, suggesting $T_c = 0$ K) and the shape of scaling function resembles the $T > T_g$ curve in Fig. 6 [21]. (Let us note that avoiding the $T < T_g$ region in the measurements of critical exponents — and in the numerical simulations as well — partially comes from the aforementioned fact that it is difficult to achieve the state of thermal equilibrium below T_g [18].) Taking all these into account, the scaling presented here for LSCNO does not exclude the possible 2D character of the SG phase in this system. In the single crystals of LSCO with $x = 0.04$ Sr concentration similar scaling was found, but splitting between ZFC and FC $\chi(T)$ curves was observed both when field was applied in Cu–O planes and along c axis, perpendicular to Cu–O planes [16]. In the single crystals of $La_{2-x}Sr_xNiO_4$ (LSNO) a splitting, indicative of SG behavior, was found only when field was applied parallel to the Ni–O planes and was not observed when the field was along c-axis, which strongly suggests that the SG phase has quasi-2D character and is related to frustration of the magnetic order in Ni–O planes [23]. In addition, the decay of remnant magnetization in LSCNO appeared to be not consistent with the stretched exponential formula while in LSCO was found to be well described by this expression with the parameter $1-n$ equal to $1/3$, the value predicted by numerical simulation for *3-dimensional* Ising SG [15]. The same value of $1 - n$ found by us in LSCNO can suggest that the mechanism of frustration in LSCNO system with substantial Cu concentration is different from this for pure nicklate. However, only measurements on single crystals of LSCNO, unavailable so far for such high Ni concentration, could definitely resolve the problem of dimensionality of the SG phase found here in this system.

4. Conclusions

In conclusion, we have studied in detail the magnetic behavior of LSCO doped with Ni. Ni frustrates the AF order in the Cu–O planes, probably even at its smallest concentration, in the superconducting phase of LSCNO. The found phase exhibits all the features that characterize a spin glass: irreversibility, remnant magnetization, and scaling behavior. The measured parameters do not exclude the presence of spin clusters. The study reveals that magnetic nature of Ni impurity in high-T_C superconductors should not be neglected even for the Ni concentration smaller than the hole concentration in the system, at least for LSCO.

Acknowledgments

This work was supported by funds of the Ministry of Science and Higher Education (Poland) as a research project for years 2007–2010 (grant No. N202 048 32/1183).

References

[1] E.W. Hudson, K.M. Lang, V. Madhavan, S.H. Pan, H. Eisaki, S. Uchida, J.C. Davis, *Nature* **411**, 920 (2001).

[2] A.V. Pimenov, A.V. Boris, L. Yu, V. Hinkov, T. Wolf, J.L. Tallon, B. Keimer, C. Bernhard, *Phys. Rev. Lett.* **94**, 227003 (2005).

[3] T. Nakano, N. Momono, T. Nagata, M. Oda, M. Ido, *Phys. Rev. B* **58**, 5831 (1998).

[4] H. Hiraka, D. Matsumura, Y. Nishihata, J. Mizuki, K. Yamada, *Phys. Rev. Lett.* **102**, 037002 (2009).

[5] C. Jaeger, C. Bihler, T. Vallaitis, S.T.B. Goennenwein, M. Opel, R. Gross, M.S. Brandt, *Phys. Rev. B* **74**, 045330 (2006).

[6] J.A. Mydosh, *Spin Glasses: An Experimental Introduction*, Taylor and Francis Ltd., London 1993.

[7] N. Marcano, J.C.G. Sal, J.I. Espeso, L.F. Barquín, C. Paulsen, *Phys. Rev. B* **76**, 224419 (2007).

[8] M. Giot, A. Pautrat, G. André, D. Saurel, M. Hervieu, J. Rodriguez-Carvajal, *Phys. Rev. B* **77**, 134445 (2008).

[9] E. Pytte, Y. Imry, *Phys. Rev. B* **35**, 1465 (1987).

[10] K. Binder, A.P. Young, *Rev. Mod. Phys.* **58**, 801 (1986).

[11] L.B.J.L. Dormann, D. Fiorani, *J. Phys. C, Solid State Phys.* **21**, 2015 (1988).

[12] C.A.M. Mulder, A.J. van Duyneveldt, J.A. Mydosh, *Phys. Rev. B* **23**, 1384 (1981).

[13] D.X. Li, T. Yamamura, S. Nimori, K. Yubuta, Y. Shiokawa, *Appl. Phys. Lett.* **87**, 142505 (2005).

[14] M.A. Continentino, A.P. Malozemoff, *Phys. Rev. B* **33**, 3591 (1986).

[15] A.T. Ogielski, *Phys. Rev. B* **32**, 7384 (1985).

[16] F.C. Chou, N.R. Belk, M.A. Kastner, R.J. Birgeneau, A. Aharony, *Phys. Rev. Lett.* **75**, 2204 (1995).

[17] L.P. Lévy, A.T. Ogielski, *Phys. Rev. Lett.* **57**, 3288 (1986).

[18] K.H. Fischer, J. Hertz, *Spin Glasses*, Cambridge University Press, Cambridge 1991.

[19] M. Suzuki, *Prog. Theor. Phys.* **58**, 1151 (1977).

[20] B. Barbara, A.P. Malozemoff, Y. Imry, *Phys. Rev. Lett.* **47**, 1852 (1981).

[21] C. Dekker, A.F.M. Arts, H.W. de Wijn, *Phys. Rev. B* **38**, 8985 (1988).

[22] W. Kinzel, K. Binder, *Phys. Rev. B* **29**, 1300 (1984).

[23] P.G. Freeman, A.T. Boothroyd, D. Prabhakaran, J. Lorenzana, *Phys. Rev. B* **73**, 014434 (2006).